

## THE THERMAL MEMORY OF REIONIZATION HISTORY

LAM HUI<sup>1,2</sup> AND ZOLTÁN HAIMAN<sup>3</sup>  
 Received 2003 April 7; accepted 2003 May 29

### ABSTRACT

The recent measurement by *WMAP* of a large electron-scattering optical depth  $\tau_e = 0.17 \pm 0.04$  is consistent with a simple model of reionization in which the intergalactic medium (IGM) is ionized at redshift  $z \sim 15$  and remains highly ionized thereafter. Here we show that existing measurements of the IGM temperature from the Ly $\alpha$  forest at  $z \sim 2$ –4 rule out this “vanilla” model. Under reasonable assumptions about the ionizing spectrum, as long as the universe is reionized before  $z = 10$  and remains highly ionized thereafter, the IGM reaches an asymptotic thermal state that is too cold compared to observations. To simultaneously satisfy the cosmic microwave background and Ly $\alpha$  forest constraints, the reionization history must be complex: reionization begins early at  $z \gtrsim 15$ , but there must have been significant (order-of-unity) changes in fractions of neutral hydrogen and/or helium at  $6 < z < 10$  and/or singly ionized helium at  $4 < z < 10$ . We describe a physically motivated reionization model that satisfies all current observations. We also explore the impact of a stochastic reionization history and show that a late epoch of (He II  $\rightarrow$  He III) reionization induces a significant scatter in the IGM temperature, but the scatter diminishes with time quickly. Finally, we provide an analytic formula for the thermal asymptote and discuss possible additional heating mechanisms that might evade our constraints.

*Subject headings:* cosmic microwave background — cosmology: theory — intergalactic medium — quasars: absorption lines

*On-line material:* color figures

### 1. INTRODUCTION

The detection by the *Wilkinson Microwave Anisotropy Probe* (*WMAP*) of a large optical depth  $\tau_e$  to electron scattering has opened a new window of studies of the ultrahigh redshift ( $z \sim 15$ ) universe (Kogut et al. 2003; Spergel et al. 2003). Taking the value  $\tau_e = 0.17 \pm 0.04$ , inferred from the polarization and temperature anisotropies of the cosmic microwave background (CMB), at face value implies that the reionization of the universe must begin very early.

The optical depth to electron scattering is given by

$$\tau_e = \int_0^\infty \frac{dz}{(1+z)H(z)} \sigma_T n_e(z) \quad (1)$$

(see, e.g., Dodelson 2003), where  $H(z)$  is the Hubble parameter at redshift  $z$ ,  $\sigma_T$  is the Thomson cross section, and  $n_e(z)$  is the proper free-electron density. This can be rewritten as

$$\tau_e = 0.0691 \Omega_b h \int_0^\infty \frac{(1+z)^2 dz}{\sqrt{\Omega_m (1+z)^3 + \Omega_\Lambda}} \quad (2)$$

$$\times \left[ (1 - Y_P) X_{\text{H II}} + \frac{1}{4} Y_P (X_{\text{He II}} + 2X_{\text{He III}}) \right],$$

where  $\Omega_b$  and  $\Omega_m$  are the baryon and matter densities, respectively, in a fraction of the critical,  $h$  is the Hubble constant in units of  $100 \text{ km s}^{-1} \text{ Mpc}^{-1}$ , and  $Y_P = 0.244 \pm 0.002$  is the helium mass fraction (Burles, Nollett, & Turner 2001). The fractions of ionized hydrogen  $X_{\text{H II}}$ , singly ionized

helium  $X_{\text{He II}}$ , and doubly ionized helium  $X_{\text{He III}}$  are functions of  $z$ .

Ignoring helium, the observed  $\tau_e = 0.17 \pm 0.04$  is consistent with a universe in which  $X_{\text{H II}}$  changes from essentially zero to close to unity at  $z = 17 \pm 3$  and  $X_{\text{H II}} \sim 1$  thereafter (Kogut et al. 2003). If helium is fully ionized together with hydrogen, the reionization redshift changes slightly to  $z = 15.3 \pm 2.7$ .<sup>4</sup>

Two features are noteworthy. First, helium reionization has a subdominant effect on  $\tau_e$  compared to hydrogen. Second, since the electron-scattering optical depth is controlled by the free-electron density, it is insensitive to the neutral fractions of hydrogen ( $X_{\text{H I}} = 1 - X_{\text{H II}}$ ) and helium ( $X_{\text{He I}} = 1 - X_{\text{He II}} - X_{\text{He III}}$ ), as long as they are small.

In contrast, the (hydrogen) Ly $\alpha$  optical depth, inferred from the spectra of distant quasars, is extremely sensitive to small amounts of neutral hydrogen. The Ly $\alpha$  optical depth at mean density is

$$\tau_\alpha = 41.8 \left[ \frac{X_{\text{H I}}}{10^{-4}} \right] \left[ \frac{1+z}{7} \right]^3 \left[ \frac{H(z=6)}{H(z)} \right] \quad (3)$$

(Gunn & Peterson 1965). Whether  $X_{\text{H I}}$  is  $10^{-4}$  or  $10^{-5}$ , for instance, makes a big difference to  $\tau_\alpha$ . Using a model for large-scale structure in the intergalactic medium (IGM), the observed mean Ly $\alpha$  transmission at  $z \sim 6$  (or the lack thereof, i.e., the Gunn-Peterson trough; Becker et al. 2001) implies a  $(1 \sigma)$  lower limit on the hydrogen neutral fraction for a fluid element at mean density:  $X_{\text{H I}} > 10^{-4}$ . The analog for Ly $\beta$  provides a stronger constraint due to the smaller absorption cross section:  $X_{\text{H I}} > 5 \times 10^{-4}$  (taken from Lidz

<sup>1</sup> Theoretical Astrophysics Department, Fermi National Accelerator Laboratory, P.O. Box 500, 500 Wilson Road, Batavia, IL 60510; lhui@fnal.gov.

<sup>2</sup> Department of Astronomy and Astrophysics, University of Chicago, 5640 South Ellis Avenue, Chicago, IL 60637.

<sup>3</sup> Department of Astronomy, Columbia University, 550 West 120th Street, New York, NY 10027; zoltan@astro.columbia.edu.

<sup>4</sup> Throughout this paper, we adopt  $\Omega_b h^2 = 0.024$ ,  $\Omega_m h^2 = 0.14$ , and  $h = 0.72$ , the central best-fit values measured by *WMAP* (Spergel et al. 2003).

et al. 2002; see also Cen & McDonald 2002; Fan et al. 2002).<sup>5</sup>

Taken at face value, these two separate observations are therefore consistent with the simplest “vanilla” model, in which the universe is reionized in a single step: the neutral fraction experiences a drop of the order of unity at  $z \gtrsim 15$ , and it remains  $\ll 1$  thereafter. Our goal in this paper is to confront this model with other existing observations and see if additional constraints can be put on the reionization history of our universe.

Several authors have pointed out that the *evolution* of the Ly $\alpha$  optical depth suggests that reionization might take place not much earlier than  $z \sim 6$  (Becker et al. 2001; Djorgovski et al. 2001; Cen & McDonald 2002; Gnedin 2001; Razoumov et al. 2002; but see also Barkana 2002; Songaila & Cowie 2002). This is based on an extrapolation of the mean transmission measurements from lower redshifts. The small number of lines of sight used (a single quasar was employed for the measurement at  $z \sim 6$ , but see Fan et al. 2003 for three new  $z > 6$  sources with Gunn-Peterson troughs) and the challenge of sky subtraction and continuum extrapolation in Gunn-Peterson trough measurements (see discussion in Becker et al. 2001; see also Hui et al. 2001), as well as our still maturing understanding of radiative transfer during reionization motivate, us to look for other clues for a late period of reionization.

The main idea is quite simple. Reionization typically heats up the IGM to tens of thousands of degrees, and the gas subsequently cools because of the expansion of the universe as well as other processes. If the universe was reionized early and has stayed highly ionized thereafter, photoionization heating of the gas cannot overcome the overall cooling, and the IGM might reach too low a temperature at low redshifts compared to observations. This idea is not new (see, e.g., Miralda-Escudé & Rees 1994; Hui & Gnedin 1997; Haehnelt & Steinmetz 1998; Theuns et al. 2002a).<sup>6</sup> Theuns et al. (2002a, 2002b), in particular, deduced a limit on the reionization redshift ( $z < 9$ ) based on temperature measurements by Schaye et al. (2000, hereafter ST00), assuming a quasar-like ionizing spectrum, and they deduced that He II reionization occurs at  $z \sim 3$ . Our objectives here are to seek a formulation of this argument that is as clean and robust as possible and reveals clearly the underlying assumptions and to check the consistency with the IGM temperatures of specific models that produce the high value of  $\tau_e$  measured by *WMAP*.

The Ly $\alpha$  forest temperature measurements we use are taken from Zaldarriaga, Hui, & Tegmark (2001, hereafter ZHT01):  $T_0 = (2.1 \pm 0.9) \times 10^4$  K at  $z = 2.4$ ,  $(2.3 \pm 0.7) \times 10^4$  K at  $z = 3$ , and  $(2.2 \pm 0.4) \times 10^4$  K at  $z = 3.9$ . Note that  $2 \sigma$  error bars are quoted, and the temperature  $T_0$  was derived for fluid elements at the mean density, consistent with our modeling of the IGM temperature in the rest of this paper. There have been several other measurements in

the past (Ricotti, Gnedin, & Shull 2000; ST00; Bryan & Machacek 2000; McDonald et al. 2001, hereafter MM01; Meiksin, Bryan, & Machacek 2001). The ones that are easiest to compare, because they are based on very similar data sets, are ST00, MM01, and ZHT01. The first two are based on line width measurements, while the last one makes use of the small-scale transmission power spectrum. A virtue of the last method is that the temperature constraints come from marginalizing over a wide array of parameters, including the slope and amplitude of the primordial power spectrum (see, e.g., Hui & Rutledge 1999) and the equation-of-state index. It is reassuring that MM01 and ZHT01, using very different methods and employing different simulations (MM01 using hydrodynamic simulations and ZHT01 using *N*-body simulations with a marginalized smoothing to mimic Jeans smoothing), agree well with each other. The results of ST00 are somewhat discrepant from these two works—the reader is referred to ZHT01 for further discussions.

An important issue in determining the temperature of the IGM is the second ionization of helium (He II  $\rightarrow$  He III). As we see, this can be an important source of heating at low redshifts,  $z \sim 3$ –4. There are several lines of evidence that suggest that He II might be reionized at  $z \sim 3$ , including observations of He II patches that do not seem to correlate with H I absorption (Reimers et al. 1997; Anderson et al. 1999; Heap et al. 2000; Kriss et al. 2001; Jakobsen et al. 2003), an increase in the IGM temperature (ST00; Theuns et al. 2002a), the evolution of the hardness of the ionizing background spectrum (Songaila 1998), and evolution of the mean transmission (Bernardi et al. 2003). On the other hand, it is unclear if the fluctuations in He II absorption observed in a few lines of sight might not be due to a naturally fluctuating IGM (Miralda-Escudé, Haehnelt, & Rees 2000). The IGM temperature measurements by MM01 and ZHT01 are consistent with no feature at  $z \sim 3$ ; power spectrum evolution also seems to argue against He II reionization at  $z \sim 3$  (P. McDonald & U. Seljak 2002, private communication). In this paper, when we consider constraints from the temperature measurement, primarily at  $z = 3.9$ , we therefore leave two options open: He II can be ionized or not ionized by  $z = 3.9$ . With this explained, we can now state our vanilla model in more concrete terms. It has two variants: (1) both hydrogen and helium are fully reionized at  $z \gtrsim 15$ , and they remain highly ionized thereafter; (2) the same as (1), except that helium is only singly ionized and remains so until at least past  $z = 3.9$ .

The paper is organized as follows. In § 2, we explain the idea of a thermal asymptote for the IGM and use it to derive a constraint on the hardness of the ionizing spectrum if the universe were to reionize before  $z = 10$  and remain highly ionized thereafter. In § 3, we discuss limits on the hardness of the ionizing spectra and show that these spectra fall short of making the thermal asymptote sufficiently hot to match observations. We then work out illustrative examples in § 4 of how order-of-unity changes in the neutral fractions at  $z \lesssim 10$  can reproduce the temperature measurements, while being consistent with the *WMAP* data. We go on to offer a physically motivated model in § 5 and discuss the implications of the fact that different fluid elements are reionized at different times (stochastic reionization). We conclude in § 6. There is in the Appendix a brief description of the thermal and chemical evolution equations that are solved numerically in our investigation.

<sup>5</sup> Note that some authors quote volume- or mass-weighted neutral fractions. We here use the neutral fraction for a fluid element that happens to be at the cosmic mean density, motivated by the fact that we discuss the temperature evolution of fluid elements with the same property in this paper.

<sup>6</sup> See also the talk by L. Hui in the 2000 Galaxy Formation and Evolution Conference, available at [http://online.kitp.ucsb.edu/online/galaxy\\_c00/hui](http://online.kitp.ucsb.edu/online/galaxy_c00/hui).

## 2. THERMAL ASYMPTOTICS

Several thermal processes are at work in a photoionized IGM. They are described in detail in Hui & Gnedin (1997). Here is a brief qualitative summary:

1. *Adiabatic heating/cooling.*—Gas elements can heat up or cool simply because of adiabatic contraction or expansion. The overall expansion of the universe drives a temperature falloff as  $(1+z)^2$  as  $z$  decreases.

2. *Photoionization heating.*—Photons inject energy into the gas by ionizing hydrogen or helium.

3. *Recombination cooling.*—Protons and electrons (or ionized helium and electrons) can cool by recombining and radiating energy away.

4. *Compton cooling.*—At sufficiently high redshifts,  $z \gtrsim 10$ , Compton scattering of free electrons with the lower temperature CMB can be an important source of cooling.

Typically, photoionization heating provides the dominant source of heating for the tenuous IGM. This occurs in primarily two forms. One is during what we call reionization “events”—these are (possibly extended) periods in which a given gas element experiences order-of-unity changes in the fractions of H I/He I/He II. The other is photoheating for an already highly ionized plasma—this occurs through photoionization of small amounts of H I/He I/He II, whose abundances are determined by photoionization equilibrium. The former provides a big boost to the temperature, while the latter determines the asymptotic thermal state of the IGM. Typical temperature evolutions are illustrated in several toy models in Figure 1.

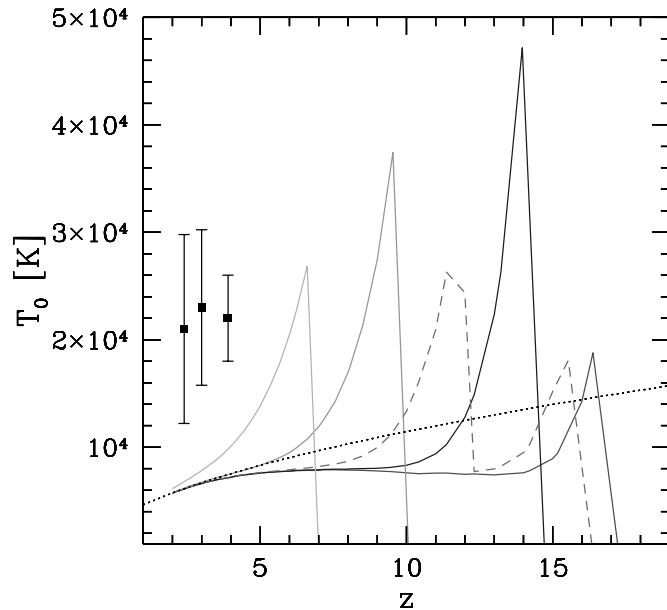


FIG. 1.—Thermal asymptote (dotted line; eq. [4]), illustrating the fact that a wide range of ionization histories results in the same IGM temperature by redshift  $z = 4$ , unless reionization occurs late. Each solid line describes the evolution of the temperature ( $T_0$ ) for a fluid element at mean density, according to a different reionization history (and a different initial reheating temperature). The dashed line illustrates the thermal evolution for a complex reionization history—such complexities do not stop the temperature from reaching the late-time asymptote, as long as they take place early, before  $z \sim 10$ . The points with  $(2\sigma)$  error bars on the left are measurements of  $T_0$  from the Ly $\alpha$  forest (ZHT01). [See the electronic edition of the Journal for a color version of this figure.]

Figure 1 shows the evolution in temperature  $T_0$  for a fluid element at mean density, with a variety of reionization histories. These histories have different reionization redshifts and initial temperature jumps, selected here only for illustration. The code for computing the thermal and chemical evolution is briefly described in the Appendix and is described in more detail in Hui & Gnedin (1997). For each thermal curve, one can see a rise to high temperatures after a reionization event. Thereafter, the varieties of reionization histories and initial reheating temperatures all result in a rather similar late-time thermal asymptote (dotted line). In fact, if reionization occurs before  $z \sim 10$  (and the IGM stays highly ionized since, or to use our earlier terminology, no reionization events take place thereafter), the temperature is always very close to the asymptote for  $z < 4$ , which is where temperature measurements exist (points with error bars). This is true even if reionization is not a single-step process, as illustrated by the dashed line, as long as complexities in the reionization process occur before  $z \sim 10$ . The term “complexities” here has a rigorous meaning: it refers to two or more episodes during which the neutral fractions of hydrogen and/or helium undergo changes of the order of unity. In all thermal curves shown in Figure 1, with one exception, such changes take place before about  $z \sim 10$ . The exception, i.e., the leftmost curve, where reionization takes place at  $z \sim 7$ , is also the only one where the asymptote is *not* reached by  $z = 4$ —this is because there is not sufficient time for the IGM to cool after a recent episode of reionization.

Figure 1 therefore illustrates two very important general facts:

1. The thermal state at  $z \leq 4$  does not remember the part of reionization history prior to  $z \sim 10$ .
2. The IGM does, however, retain short-term memory of reionization events in its recent past.

What determines the late-time thermal asymptote? It is the combination of photoionization heating, recombination cooling, and adiabatic cooling. An approximate analytic expression can be derived for the thermal evolution of the IGM (Hui & Gnedin 1997). We find that the following simple formula provides a more accurate ( $\sim 5\%$ ) fit to the numerically computed thermal asymptote (for  $T_0$  at  $z = 2-4$ ), for a variety of spectral shapes we have tested:

$$T_0 = [B(1+z)^{0.9}]^{1/1.7}, \quad (4)$$

where

$$B \equiv 18.8 \text{ K}^{0.7} \left[ \sqrt{\frac{0.14 \Omega_b h^2}{\Omega_m h^2 0.024}} \right] \times \left( T_{\text{HI}} + \frac{X_{\text{HeII}}}{16} T_{\text{HeI}} + \frac{5.6 X_{\text{HeIII}}}{16} T_{\text{HeII}} \right), \quad (5)$$

$$T_i \equiv k_B^{-1} \frac{\int_{\nu_i}^{\infty} J_\nu \sigma_i (h\nu - h\nu_i) d\nu / (h\nu)}{\int_{\nu_i}^{\infty} J_\nu \sigma_i d\nu / (h\nu)}.$$

Here  $k_B$  is Boltzmann’s constant, the symbol  $J_\nu$  denotes the ionizing intensity as a function of frequency (in units of energy per frequency per time per area per steradian),  $\sigma_i$  denotes the ionization cross section for the respective species ( $i = \text{H I}, \text{He I}, \text{or He II}$ ),  $\nu_i$  is the ionizing threshold frequency, and  $h$  is the Planck constant (in distinction from the

Hubble constant  $h$ ). It is useful to remember that  $h\nu_{\text{HI}}/k_{\text{B}} = 1.57807 \times 10^5 \text{ K}$ ,  $\nu_{\text{He I}} = 1.808\nu_{\text{HI}}$ , and  $\nu_{\text{He II}} = 4\nu_{\text{HI}}$ .

The asymptote given in equation (4) assumes that at late times, hydrogen is highly ionized. That is why the term due to photoheating of H I,  $T_{\text{HI}}$ , has the form shown in equation (5). The denominator of  $T_{\text{HI}}$ , when multiplied by  $4\pi$ , is the photoionization rate of neutral hydrogen—its inverse is hence proportional to the (small) hydrogen neutral fraction under ionization equilibrium. Its numerator gives the photoheating rate per neutral atom. The combination of factors in  $T_{\text{HI}}$  therefore gives a temperature scale whose amplitude is proportional to the net amount of H I photoheating. Similarly, the terms  $X_{\text{He II}}T_{\text{He I}}/16$  and  $5.6X_{\text{He III}}T_{\text{He II}}/16$  in equation (5) quantify the importance of photoheating of He I and He II, respectively. The factors of  $X_{\text{He II}}$  and  $X_{\text{He III}}$  arise because of photoionization equilibrium. If, asymptotically, helium is doubly (singly) ionized, then  $X_{\text{He II}}$  ( $X_{\text{He III}}$ ) can be set to zero.

It is important to emphasize that the thermal asymptote given in equation (4) is determined completely by the shape (or “hardness”) of the ionizing spectrum  $J_\nu$ , but not its amplitude. For a power-law  $J_\nu \propto \nu^{-\alpha}$ , the thermal asymptote can be recast simply as

$$T_0 = 2.49 \times 10^4 \text{ K} (2 + \alpha)^{-1/1.7} \left( \frac{1+z}{4.9} \right)^{0.53}, \quad (6)$$

assuming, asymptotically, that helium is doubly ionized.

Given the above, we can ask the following question: How hard does the ionizing spectrum have to be for the thermal asymptote to match the observed temperatures at low redshifts? It suffices to use the measurement at the highest redshift,  $z = 3.9$ :  $T_0 = (2.2 \pm 0.4) \times 10^4 \text{ K}$  ( $2 \sigma$  error bar; ZHT01). More concretely, what constraint can be placed on  $\alpha$  if the thermal asymptote were to reach  $T_0 > 1.6 \times 10^4 \text{ K}$  ( $3 \sigma$  lower limit) by  $z = 3.9$ ? It is straightforward to show that this requires  $\alpha < 0.12$ , from equation (6).

One can also derive a similar limit if it is assumed that helium is only singly ionized by  $z = 3.9$  ( $X_{\text{He II}} \sim 1$ ). Assuming again a power-law  $J_\nu \propto \nu^{-\alpha}$ , but with a cutoff for  $\nu > \nu_{\text{He II}}$ , the requirement is  $\alpha < -2.2$ .<sup>7</sup> In other words, the spectrum needs to be even harder with no He II photoheating, and a spectrum as hard as  $\alpha < -2.2$  is unrealistic compared to stellar and quasar spectra.

To summarize, if reionization takes place at  $z > 10$  and the fractions of H I/He I/He II experience no significant (order-of-unity) change after  $z = 10$ , a sufficiently hard ionizing spectrum is necessary to keep the IGM temperature high enough to match observations at  $z = 3.9$ . Parameterizing the ionizing background by a power law  $J_\nu \propto \nu^{-\alpha}$ , this requires  $\alpha < 0.12$  if He II is reionized by  $z = 3.9$  or  $\alpha < -2.2$  if He II is not reionized by then (the latter assumes that  $J_\nu$  is cut off for  $\nu > \nu_{\text{He II}}$ ). One should keep in mind that the only relevant slope of the spectrum is the slope just above each ionization threshold (unless the spectrum is very hard), because the ionization cross section  $\sigma_i \sim \nu^{-3}$ . In other words,  $\alpha$  can deviate greatly from the values given above as long as the deviation takes place at frequencies far away from the ionization thresholds. Note also that the spectrum described here refers to the asymptotic spectrum at  $z = 3.9$ .

<sup>7</sup> A slope of  $-2.2$  appears unphysical, but the only relevant slope as far as photoheating is concerned is the one just above the ionizing threshold; see further comments in the next paragraph.

If the spectrum changes significantly after  $z \sim 10$ , one can view the above limits as applicable to the hardest spectrum between  $z = 3.9$  and 10.

The power index we find,  $\alpha < 0.12$  or  $< -2.2$ , represents a very hard spectrum. We next turn to the following question: How hard can a realistic ionizing spectrum be?

### 3. THE IONIZING SPECTRUM

Two kinds of ionizing spectra are generally discussed in the literature. One is quasar-like, and the other is starlike.

Zheng et al. (1998) finds a quasar spectral shape of  $\sim \nu^{-1.8}$  for the relevant ionizing frequencies in high-resolution *Hubble Space Telescope* spectra. In this paper, we follow Haardt & Madau (1996) and consider, conservatively, a quasar spectrum that goes as  $\nu^{-1.5}$ . One should keep in mind that, at the relevant redshifts  $\gtrsim 4$ , the known populations of quasars probably cannot contribute significantly to the (hydrogen) ionizing background. Here we take the conservative view that there might be a population of dim quasars that still contributes significantly to a hard spectrum (Haiman & Loeb 1997).

Stellar spectra are generally softer than a typical quasar spectrum. An exception is the spectra of metal-free stars (Tumlinson & Shull 2000; Bromm, Kudritzki, & Loeb 2001; Schaerer 2002; Venkatesan, Tumlinson, & Shull 2003). In their theoretical models, Bromm et al. (2001) find a spectrum that has the following form:  $J_\nu \sim \nu$  for  $\nu$  just above  $\nu_{\text{HI}}$ ,  $J_\nu \sim \nu^0$  at  $\nu \gtrsim \nu_{\text{He I}}$ , and  $J_\nu \sim \nu^{-4.5}$  for  $\nu \gtrsim \nu_{\text{He II}}$ . Such a spectrum is harder than the quasar spectrum at frequencies below the He II threshold. Note that metal-free stars probably cause reionization early on, but it is unlikely that they contribute significantly to the asymptotic ionizing spectrum at low redshifts (Haiman & Holder 2003). We consider a metal-free stellar spectrum here for the sake of being conservative; i.e., we assume a spectrum that is as hard as possible.

The actual ionizing spectrum seen by a fluid element is different from the above because of processing by the IGM. Haardt & Madau (1996) have done a careful calculation of such effects. Absorption generally hardens the spectrum.<sup>8</sup> However, diffuse recombination radiation from the absorbing medium tends to compensate for this hardening. Haardt & Madau (1996) found that the spectrum above  $\nu_{\text{He II}}$  hardens by 1.5 (to be precise,  $\alpha \rightarrow \alpha - 1.5$ ; see also Zuo & Phinney 1993). The spectrum just above  $\nu_{\text{HI}}$  and  $\nu_{\text{He I}}$  maintains roughly the same slope as the source.

We are therefore led to consider the following IGM modified spectra. Let us use the symbols  $\alpha_{\text{HI}}$ ,  $\alpha_{\text{He I}}$ , and  $\alpha_{\text{He II}}$  to denote the spectral slopes (more precisely, their negative) above the three relevant ionizing thresholds. A quasar-like processed spectrum has  $\alpha_{\text{HI}} = \alpha_{\text{He I}} = 1.5$  and  $\alpha_{\text{He II}} = 0.0$ . A metal-free stellar spectrum gives rise to  $\alpha_{\text{HI}} = -1$ ,  $\alpha_{\text{He I}} = 0$ , and  $\alpha_{\text{He II}} = 3$ . At the moment(s) of reionization, the relevant spectrum can, however, be even harder (Abel & Haehnelt 1999). In principle, the spectrum can be hardened relative to the source by as much as a power-law index of 3, the 3 coming from the scaling  $\sigma_i \propto \nu^{-3}$  (see arguments in Abel & Haehnelt 1999 and also Zuo & Phinney 1993). We

<sup>8</sup> Note the apparent paradox: absorption, by taking away ionizing photons, *increases* the photoheating rate. This is a result of photoionization equilibrium, which makes the amplitude of the ionizing background irrelevant (eq. [5]). Rather, it is the spectral shape that is important.

therefore allow the quasar spectrum to have  $\alpha_{\text{H I}} = \alpha_{\text{He I}} = \alpha_{\text{He II}} = -1.5$  and the stellar spectrum to have  $\alpha_{\text{H I}} = -4$ ,  $\alpha_{\text{He I}} = -3$ , and  $\alpha_{\text{He II}} = 1.5$  at the initial moment(s) of reionization. This is not relevant for the thermal asymptote, but is relevant for the magnitude of temperature boosts during reionization events.

Comparing the above spectral slopes against the limits obtained in the last section suggests that neither quasars nor metal-free stars can match the observed temperature at  $z = 3.9$ , if reionization occurs at  $z > 10$  and no reionization event takes place afterward. However, those limits were based on a strict power-law spectrum. The thermal asymptotes (eq. [4]) for our more realistic spectra for quasars and metal-free stars are shown in Figures 2 and 3 (*dotted lines*), respectively. Indeed, in both cases, the thermal asymptotes fall short of the observed ( $3\sigma$ ) lower limit of  $T_0 > 1.6 \times 10^4$  K at  $z = 3.9$ , regardless of whether or not helium is doubly ionized.

Hence, if the universe is reionized before  $z \sim 10$  and remains highly ionized thereafter, neither reasonably hard spectrum can reproduce the IGM temperatures inferred from the Ly $\alpha$  forest.

#### 4. ILLUSTRATIVE EXAMPLES

The conclusion from the last section, together with the large electron-scattering optical depth measured by

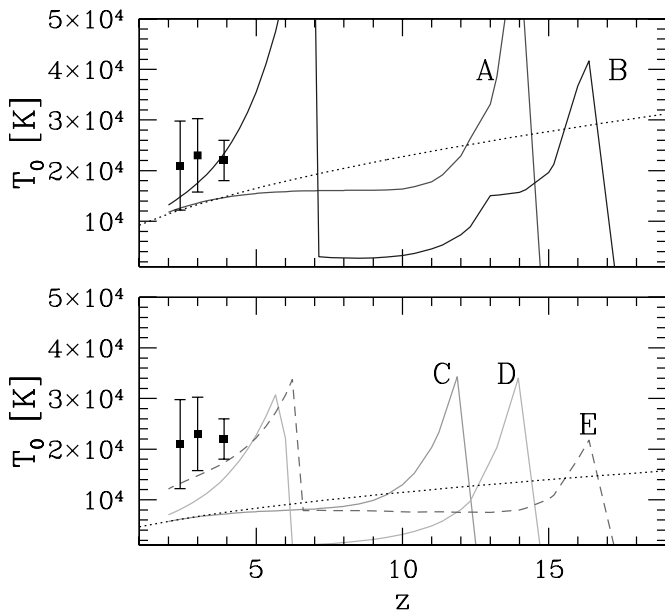


FIG. 2.—Thermal evolution for a quasar-like ionizing spectrum. *Top*: Helium is doubly ionized together with hydrogen. The dotted line shows the thermal asymptote (eq. [4]). The solid lines show the thermal evolution for two different reionization histories. Model A has a single-episode reionization at  $z = 14$  and stays highly ionized thereafter. Model B also has early reionization, but experiences a drop in ionizing flux thereafter and starts recombining until  $z \sim 7$ , at which time it undergoes a second period of hydrogen and helium (I and II) reionization. Model A, reaches a high enough  $T_0$  to match observations (points with error bars; ZHT01). *Bottom*: Helium is singly ionized together with hydrogen; the double ionization of helium is never reached (except in model E). The dotted line shows the asymptote in such a case. Models C and D (*solid lines*) are analogs of A and B above—the only difference is that here, helium remains only singly ionized. In model E (*dashed line*), hydrogen and helium are (singly) ionized at  $z \sim 17$ , and then He II is ionized at  $z \sim 6.5$ . [See the electronic edition of the Journal for a color version of this figure.]

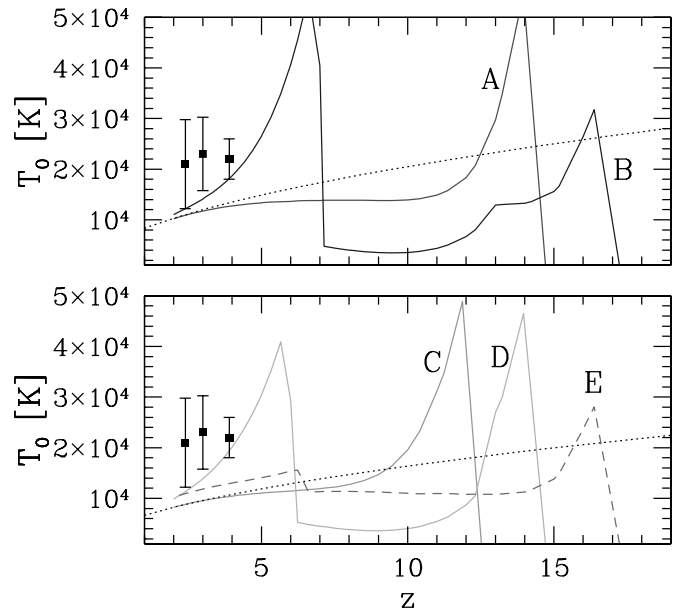


FIG. 3.—Thermal evolution using a spectrum motivated by metal-free stars. All reionization histories are exact analogs of those in Fig. 2. All symbols inherit the same meanings. [See the electronic edition of the Journal for a color version of this figure.]

*WMAP*, therefore implies that one or more of the fractions  $X_{\text{H I}}$ ,  $X_{\text{He I}}$ , or  $X_{\text{He II}}$  must change by the order of unity at  $z < 10$  to give the IGM temperature boosts above the thermal asymptote. We therefore *rule out* the vanilla reionization models laid out in § 1. One should keep in mind, however, that this is predicated on (reasonable) assumptions about the hardness of the ionizing spectrum. In this section, we work out some illustrative examples of what it takes to match the IGM temperature constraints, using the spectra from the last section.

Figure 2 shows the thermal evolution for a fluid element at mean density subject to a quasar-like ionizing spectrum and experiencing a variety of ionization histories, for the case in which helium is both doubly (*top panel*) and singly ionized (*bottom panel*, except for model E; see below). Models A and C both describe early reionization, before  $z = 10$ , and no significant (order-of-unity) changes in  $X_{\text{H I}}$ ,  $X_{\text{He I}}$ , or  $X_{\text{He II}}$  thereafter. As explained before, both converge to their respective thermal asymptotes by  $z \sim 4$ , which falls short of the observed temperatures, especially for model C, which has no He II reionization and therefore lower temperatures. Model B demonstrates how early reionization can be made consistent with the forest temperature measurements. It has a late second episode of (both H and He I and II) reionization at  $z \sim 7$ , which boosts the temperature significantly above the thermal asymptote. Model E is similar, except that in the second episode, only He II is reionized (H I and He I were already highly ionized before then). It shows that He II reionization alone can provide a significant boost to the IGM temperature.

Model D is intriguing, as it shows a case in which a second episode of hydrogen (and He I but not He II) reionization occurs at the smallest redshift ( $z = 6$ ) allowed by Sloan Digital Sky Survey (SDSS) observations (Fan et al. 2002). Even with such a late reionization epoch, the temperature can barely match the observations (the temperature at  $z = 3.9$  is  $1.5 \times 10^4$ , which is just below the  $3\sigma$  limit). This is due to

the lack of He II reionization in this model. Therefore, with a quasar spectrum like the one assumed here, some amount of He II reionization *is necessary* prior to  $z \sim 4$  to heat the IGM sufficiently. If the evidence that suggests that He II reionization is occurring at  $z \sim 3$  holds up (see § 2), then this implies that either a spectrum harder than assumed here for quasars exists prior to  $z \sim 4$  or else He II reionization must last for an extended period, from  $z \sim 3$  back to at least  $z > 4$ . Figure 3 shows a similar exercise for a metal-free stellar spectrum (as defined in § 3). We emphasize again, however, that it is unlikely that metal-free stellar spectra remain a dominant contribution to the ionizing background down to low redshifts (Haiman & Holder 2003). This figure should only be viewed as an illustration of possibilities. The curves are exact analogs of those in Figure 2. Two features are different from the previous figure. Model E, in which a late period of He II reionization occurs around  $z \sim 6$ , can no longer heat up the IGM sufficiently to be consistent with observations. This is because of the softness of a stellar spectrum above the He II threshold. On the other hand, model D, which has a late hydrogen (and He I but no He II) reionization at  $z \sim 6$ , has no problem matching the observed temperatures, unlike its quasar analog shown in Figure 2. This is because the stellar spectrum we adopted is, in fact, harder than the quasar spectrum for frequencies just above  $\nu_{\text{H I}}$  and  $\nu_{\text{He I}}$ . Finally, before we move on to the next section, it is interesting to explore a situation that is intermediate between the two extremes we have considered above; i.e., He II is partially ionized early on and stays partially ionized thereafter. Because the recombination rate of He III to He II is high, one might wonder if the continuous photoionization and recombination could give rise to a sufficiently high temperature.<sup>9</sup> We show in Figure 4 the thermal evolution (*top panel*) for a fluid element that experiences reionization at  $z > 10$ , with the He II fraction (*bottom panel*) maintaining at the 80% level thereafter. The thermal evolution assumes a quasar spectrum identical to that used in Figure 2 (in particular,  $\alpha_{\text{He II}} = 0$  for the processed, post-reionization spectrum; see § 3), except that a break in the ionizing flux just above the He II threshold is tuned to give rise to  $X_{\text{He II}} \sim 0.8$ . Notice how the analytic asymptote (*dotted line*; from eq. [4], with  $X_{\text{He II}} = 0.8$ , and  $X_{\text{He III}} = 0.2$ ) remains an excellent approximation to the late-time thermal evolution. One can see that the late-time temperature is intermediate between the cases of full He II reionization and no He II reionization, depicted in Figure 2. In other words, partial He II reionization is nicely bracketed by the cases we have considered already. A caveat one should keep in mind, however, is that when  $X_{\text{He II}}$  is close to unity, the processed ionizing spectrum is expected to be still harder above the He II threshold than what we have already assumed. Trying  $\alpha_{\text{He II}} = -1.5$  (which is the hardest possible; see § 3) in place of  $\alpha_{\text{He II}} = 0$  in Figure 4 results in a temperature at  $z \sim 4$  of  $1.3 \times 10^4$  K, which still falls short of the observed temperature. For smaller  $X_{\text{He II}}$ , one expects the spectrum to be softer.

## 5. STOCHASTIC REIONIZATION HISTORY: RESULTS FROM A PHYSICALLY MOTIVATED MODEL

In the above sections we have used toy models of reionization to illuminate the key issues that determine the tem-

<sup>9</sup> We thank Andrea Ferrara for posing the question.

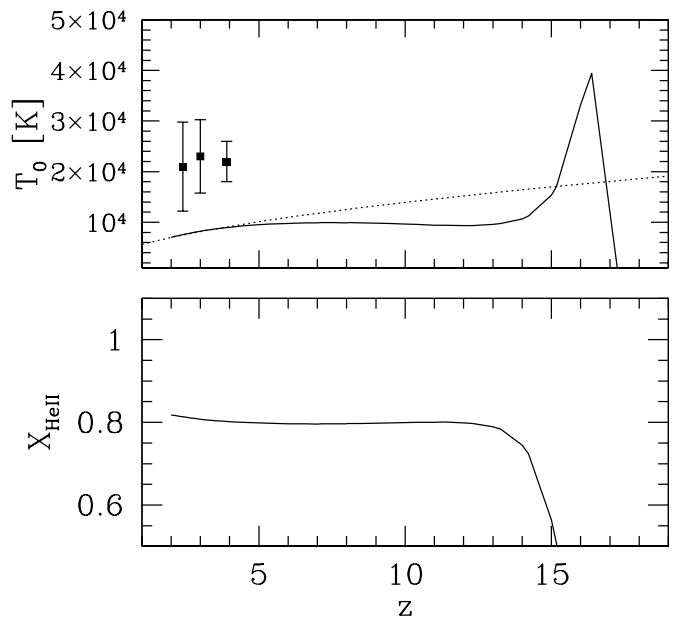


FIG. 4.—Thermal evolution (*solid line, top panel*) using the same quasar-like spectrum as is assumed in Fig. 2, except that the amplitude of the ionizing radiation just above the He II threshold is tuned to give rise to partial He II ionization (*bottom panel*). The dotted line shows the thermal asymptote given in eq. (4).

perature evolution of the IGM. It is interesting to consider this evolution in a physically motivated model of the reionization history that appears to fit all the relevant observations (including the electron-scattering optical depth  $\tau_e = 0.17$  measured by *WMAP*). Based on assumptions about the nature and efficiency of the ionizing sources, the reionization history can be predicted from “first principles” in numerical simulations (see, e.g., Gnedin & Ostriker 1997; Nakamoto, Umemura, & Susa 2001; Gnedin 2000, 2001; Razoumov et al. 2002) and in semianalytical models (see, e.g., Shapiro, Giroux, & Babul 1994; Tegmark, Silk, & Blanchard 1994; Haiman & Loeb 1997, 1998; Valageas & Silk 1999; Wyithe & Loeb 2003; Cen 2003). Here we consider a semianalytical model adopted from Haiman & Holder (2003), but modified to include the ionization of He II  $\rightarrow$  He III. For technical details, the reader is referred to that paper. Inclusion of He III is conceptually straightforward.

In this model, we follow the volume filling fractions  $x_{\text{H II}}$  and  $x_{\text{He III}}$  of H II and He III, assuming that discrete, ionized Strömgen spheres are being driven into the IGM by ionizing sources located in dark matter halos. As can be seen from equation (5), photoionization of He I (to He II) plays a subdominant role in heating the IGM. For simplicity, we assume that He I is reionized at the same time as H I, so there is no need to separately keep track of the filling fraction of He I. Note that before the Strömgen spheres percolate, the radiation background is extremely inhomogeneous: fluid elements inside ionized regions see the flux of a single (or a cluster of a few) sources, whereas fluid elements in the still neutral regions see zero flux.<sup>10</sup> In this picture, each fluid

<sup>10</sup> These statements would no longer hold if the early ionizing sources had a hard spectrum extending to  $\gtrsim 1$  keV energies, an interesting possibility (see, e.g., Oh 2001; Venkatesan, Giroux, & Shull 2001) that we do not consider in this paper.

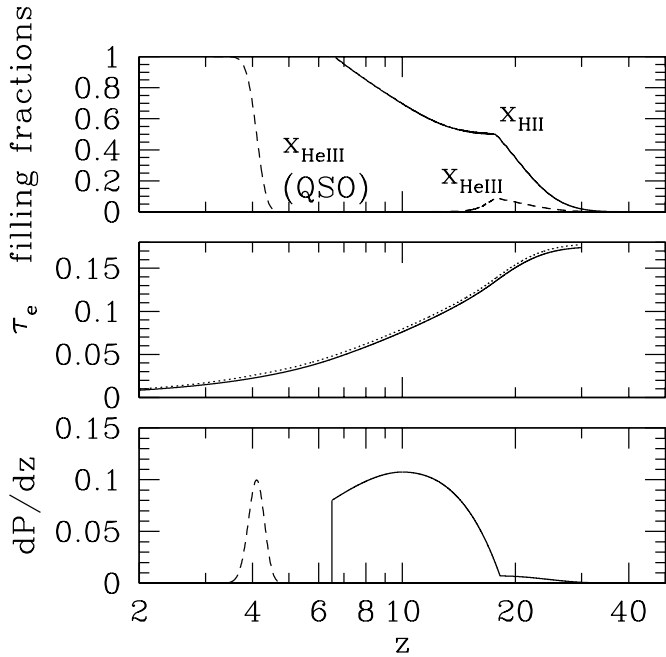


FIG. 5.—*Top:* Evolution of the volume filling fractions  $x_{\text{H II}}$  and  $x_{\text{He III}}$  of ionized hydrogen and helium in a physically motivated reionization model. The solid curve corresponds to H II and the dashed curve to He III regions. The extra dashed curve to the left (QSO) corresponds to the evolution of volume filling fraction of He III regions due to a late period of He II reionization, driven by the population of known quasars at  $z > 3$ . *Middle:* Electron-scattering optical depth, integrated from 0 to  $z$ . Two barely distinguishable curves are shown here: excluding/including free electrons from the quasar-induced He II ionization. *Bottom:* The solid curve shows the probability distribution of hydrogen reionization redshifts. The dashed curve shows the distribution of (late) He II reionization redshifts. The amplitude of the latter distribution has been divided by a factor of 20, for clarity of presentation.

element is engulfed by an ionization front at a different time. In effect, each fluid element therefore has a different reionization history. Rather than considering a single temperature for a fluid element at the mean density, it is more appropriate to consider an *ensemble* of fluid elements at the mean density, each with a different reionization history and temperature evolution. Note that this stochasticity is *in addition* to the IGM having a distribution of temperatures due to density variations (see § 6 for a discussion of the latter). The evolutions of  $x_{\text{H II}}$  and  $x_{\text{He III}}$  in our model are shown by the solid and dashed curves, respectively, in the top panel of Figure 5 (ignore the QSO curve to the left for the moment). Reionization has an interesting history that reflects contributions from three distinct types of ionizing sources and two different feedback effects (all of which have physical motivations as described in detail in Haiman & Holder 2003). In short, ionizing sources (assumed to be massive metal-free stars) first appear inside gas that cools via  $\text{H}_2$  lines and collects in the earliest nonlinear halos with virial temperature of  $100 \text{ K} \lesssim T \lesssim 10^4 \text{ K}$ . These sources ionize  $\sim 50\%$  of the volume in hydrogen, and they have sufficiently hard spectra (see discussion above) that they reionize  $\sim 10\%$  of the helium. However, at this stage (redshift  $z \sim 17$ ) the entire population of these first-generation sources effectively shuts off because of global  $\text{H}_2$  photodissociation by the cosmic soft UV background they had built up. Soon more massive halos, with virial temperatures of  $10^4 \text{ K} \lesssim T \lesssim 2 \times 10^5 \text{ K}$  form, which do not rely on  $\text{H}_2$  to cool their gas (they cool

via neutral H excitations), and new ionizing sources turn on in these halos. These are assumed to be “normal” stars, since the gas had already been enriched by heavy elements from the first generation. These sources continue ionizing hydrogen, but since they produce little flux above the He II edge, helium starts recombining. This second-generation population is also self-limiting: gas infall to these relatively shallow potential wells is prohibited inside regions that had already been ionized and photoheated to  $10^4 \text{ K}$ . As a result, hydrogen reionization starts slowing down around  $z \sim 10$  (see the solid curve in the bottom panel of Fig. 5). However, at this stage, still larger halos with virial temperatures of  $T \gtrsim 2 \times 10^5 \text{ K}$  start forming. These relatively massive, third-generation halos are impervious to photoionization feedback and complete the reionization of hydrogen.

As far as the late-time thermal state is concerned, the relevant ionizing spectrum is that of the sources that turn on after  $z \sim 17$ . These are Population II stars—a reasonable spectrum is  $\alpha_{\text{H I}} = 1$ ,  $\alpha_{\text{He I}} = 4$ , and heavily truncated beyond  $\nu_{\text{He II}}$  (Leitherer et al. 1999). As we have illustrated with examples in the last section, a spectrum as soft as this, even with some amount of late (H I and He I but not He II) reionization after  $z \sim 10$ , has difficulty heating up the IGM to high enough temperatures (even after accounting for processing of the spectrum by the IGM; see § 3).

We are therefore led to consider the effect of quasars. Sokasian, Abel, & Hernquist (2002) showed, based on a three-dimensional radiative transfer simulation, that He II reionization should occur around  $z \sim 4$ , driven by the population of known quasars.<sup>11</sup> According to this work, He II  $\rightarrow$  He III reionization is completed within a relatively short redshift range (see the left-hand dashed curve in the top panel of Fig. 5). We approximate their probability distribution of (late) He II reionization redshifts as a Gaussian centered at 4.1 with an FWHM of 0.5 (dashed curve in the bottom panel of Fig. 5). The quasar spectrum is as described in § 3.

We generate reionization histories for an ensemble of fluid elements (at mean density) in a stochastic way: determining the redshifts of H I (and He I) reionization and He II reionization by drawing from the probability distributions described in the bottom panel of Figure 5. The resulting temperatures at  $z = 2.4, 3.0$ , and  $3.9$  have a scatter because of the stochastic history, and their probability distributions are shown in Figure 6. The results shown in this figure are intriguing. At  $z = 3.9$ , the distribution (*solid histogram*) peaks around  $T_0 = 2.2 \times 10^4 \text{ K}$ , but it has a significant bump below  $10^4 \text{ K}$  as well. This bimodal distribution is a result of the stochastic reionization history: at  $z = 3.9$ , there is a minority of fluid elements that have not undergone He II reionization, and so they are significantly colder, by more than a factor of 2. There have been attempts in the past to look for temperature fluctuations (beyond what one expects from variations with density) in the Ly $\alpha$  forest (Zaldarriaga 2002; Theuns et al. 2002b). So far there has been no detection. Our results indicate that the stochasticity of reionization can detectably increase the width of the temperature distribution. It will be very interesting to confirm our results by a more detailed analysis that folds in a realistic density

<sup>11</sup> Wyithe & Loeb (2003) considered He II reionization by the known quasar population in a semianalytical model and obtained a similar result: He II reionization extends beyond  $z \sim 4$ , but is complete by around then.

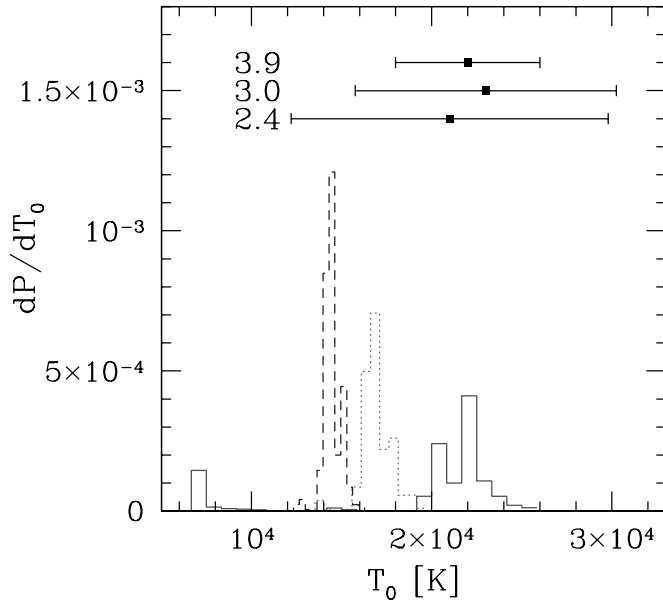


FIG. 6.—Probability distribution of temperature  $T_0$  for fluid elements at mean density, for three different redshifts  $z = 2.4$  (dashed histogram),  $3.0$  (dotted histogram), and  $3.9$  (solid histogram). The observed temperatures with their  $2\sigma$  error bars are shown at the top. [See the electronic edition of the Journal for a color version of this figure.]

distribution and to apply the observational search techniques to larger data sets and higher redshifts ( $z \sim 3$  so far).

The formal mean and rms scatter of  $T_0$  at  $z = 3.9$  is  $1.8 \times 10^4 \pm 7 \times 10^3$  K. It can be seen from Figure 6 that the scatter gets progressively smaller as one goes to lower redshifts: at  $z = 3.0$ ,  $T_0 = 1.7 \times 10^4 \pm 8 \times 10^2$  K; at  $z = 2.4$ ,  $T_0 = 1.5 \times 10^4 \pm 5 \times 10^2$  K. The scatter at these lower redshifts is no larger than the expected scatter from shock heating as well as dynamics (see, e.g., Croft et al. 1997; Hui & Gnedin 1997; Dave & Tripp 2001).

## 6. DISCUSSION

We find that the temperature of the IGM, as inferred from Ly $\alpha$  forest spectra at redshifts  $z \approx 2$ –4, leads to several interesting conclusions. Especially interesting are the conclusions we obtain when the Ly $\alpha$  forest temperature is considered together with the *WMAP* results. Our main conclusions are summarized as follows:

1. A vanilla reionization model, in which  $X_{\text{H I}}$ ,  $X_{\text{He I}}$ , and/or  $X_{\text{He II}}$  undergo order-of-unity changes at  $z > 10$ , but suffer no such changes at  $z < 10$ , is ruled out by temperature measurements of ZHT01, especially at  $z = 3.9$ . This relies on assumptions about the ionizing spectrum, which are discussed in § 3. For a power-law spectrum, rigorous requirements can be put on the hardness of the ionizing background to evade the above argument:  $\alpha < 0.12$  if helium is doubly ionized or  $\alpha < -2.2$  if helium is singly ionized, for  $J \propto \nu^{-\alpha}$  (with a cutoff at  $\nu_{\text{He II}}$  if helium is only singly ionized). The idea of an asymptotic evolution for the thermal state of the IGM is quite useful in formalizing the above argument. The asymptote (at  $2 \leq z \leq 4$ ) is described quite accurately ( $\sim 5\%$ ) by equation (4). It is reached as long as any order-of-unity changes in  $X_{\text{H I}}$ ,  $X_{\text{He I}}$ , and/or  $X_{\text{He II}}$  occur prior to  $z = 10$ .

2. Conversely, the requirement by *WMAP* that the universe reionizes early, at  $z > 10$ , implies that the reionization history is complex. To fulfill the temperature constraints, there must be additional periods of order-of-unity changes in one or more of the fractions  $X_{\text{H I}}$ ,  $X_{\text{He I}}$ , or  $X_{\text{He II}}$  at redshifts below 10. This is an argument separate from the argument based on the evolution of mean transmission (Haiman & Holder 2003; based on the Gunn-Peterson troughs observed by Becker et al. 2001 and Fan et al. 2003 at  $z \sim 6$  and a comparison against an extrapolation from lower redshifts).

3. Exactly what kind of changes at  $z < 10$  are necessary to match the temperature constraint at  $z = 3.9$  depends critically on the ionizing spectrum. If the spectrum is harder than  $\nu^{-1.5}$  above the H I and He I ionization thresholds (i.e., harder than the “quasar” spectrum discussed in § 3), then order-of-unity changes in  $X_{\text{H I}}$  and  $X_{\text{He I}}$  in the period  $6 \lesssim z \lesssim 10$  (the lower limit of 6 being set by the SDSS mean transmission measurements; Fan et al. 2002), even without accompanying changes in  $X_{\text{He II}}$  (i.e., no He II reionization), are sufficient to heat up the IGM to within the constraint at  $z = 3.9$ . Conversely, if the spectrum is not hard enough (for instance, a Population II stellar spectrum described in § 5), some amount of He II reionization heating is *necessary* prior to  $z = 3.9$ .

4. The IGM temperature can have a broad distribution (beyond what one expects based on variation with density) close to reionization events, but the scatter diminishes with time. The reionization history of the universe is almost certainly stochastic, in the sense that different fluid elements reionize at different times, depending on when a given element becomes engulfed in expanding H II (or He III) regions around ionizing sources. Based on simple semianalytic models, we predict the probability distribution of ionization redshifts. The resulting temperature scatter is particularly large close to reionization events, but diminishes quickly with time. This is illustrated in Figure 6. It would be very interesting to search for the broad initial temperature scatter that is predicted by physically motivated reionization models.

5. The known quasar population at  $z < 5$  may heat the IGM to sufficiently high temperatures by reionizing He II. In § 5, we describe a physically motivated reionization model with a stochastic history. Hydrogen (and He I) reionization is accomplished early on by metal-free stars ( $17 \lesssim z \lesssim 30$ ) and later on by Population II stars ( $z \lesssim 17$ ) and completes by  $z \sim 6.5$ . This fulfills the dual requirements of a large CMB optical depth and the Gunn-Peterson trough seen by SDSS. Because the Population II stars have a rather soft spectrum, photoheating of H I and He I alone is not enough to bring the temperature up to the observed level, and this model *fails* to predict sufficiently high IGM temperatures—despite the percolation occurring at the relatively low redshift of  $z \sim 7$ . We therefore make use of the predictions of Sokasian et al. (2002) for a brief period of He II reionization around  $z \sim 4$ , based on the *known* population of quasars. We find that such a model can satisfy the temperature constraints. It is important to note, however, that this is not the only way to achieve the observed temperatures. For instance, a population of dim quasars can turn on at  $z > 6$  (Haiman & Loeb 1997), which has a sufficiently hard spectrum to either heat the IGM via photoheating of H I and He I alone (but their spectrum has to be harder than  $\nu^{-1.5}$  if He II is not reionized) or boost the temperature via

He II reionization. If He II reionization takes place via these miniquasars, the turn-on of the known population of quasars at  $z \lesssim 4$  then has a much weaker influence on the thermal state at low redshifts.

6. He II reionization makes little difference to the electron-scattering optical depth, particularly if it occurs late. For instance, in the model shown in Figure 5, extra electrons from He II reionization change  $\tau_e$  at a 2% level fractionally.

An important caveat in our discussion so far is the possible existence of additional heating mechanisms. Two such possibilities are galactic outflows and Compton heating by a hard X-ray background. Adelberger et al. (2003) recently observed signatures of galactic winds into the IGM. Such outflows can in principle heat up the IGM. However, observations by Rauch et al. (2001) of close pairs of lines of sight in lens systems suggest that the IGM is not turbulent on small scales, arguing against significant stir-up of the IGM by winds. Moreover, galactic outflows can heat up the IGM to a variety of temperatures—the fact that the observed temperatures are in the range of expectations for a photoionized, and photoheated, gas suggests that photoheating is the simplest explanation.

Another important question is whether Compton heating by a hard X-ray background (XRB) could be more important than photoelectric heating. This question was considered by Madau & Efstathiou (1999), who assumed that the redshift evolution of the sources of the hard XRB parallels the flat distribution that had been determined for the soft X-ray AGN luminosity function beyond  $z \sim 2$ . Under this assumption, they found the hard XRB to be an important source of heating relative to the UV background at redshifts  $z > 2$ , raising the IGM temperature to  $1.5 \times 10^4$  K at  $z \sim 4$ . Two new developments make it unlikely for the hard XRB to be an important source of heating. First, as pointed out by Abel & Haehnelt (1999), the photoelectric heating rate

can be significantly increased in optically thick gas (when hydrogen and helium first gets ionized); we here adopt these increased rates. Second, the sources of the hard XRB have been resolved by the *Chandra* satellite, and, rather than paralleling the soft X-ray luminosity function, the hard X-ray sources exhibit a steep decline toward high redshift beyond  $z \sim 2$  (Cowie et al. 2003).

Our investigation raises a number of interesting issues. Is He II reionization prior to a redshift of 4 necessary to heat up the IGM to the right level? This depends critically on what kind of sources and spectra are available. The prediction for a large scatter in temperature (factor of about 2) close to the epoch of He II reionization is something one could look for, if indeed He II reionization occurs late (Zaldarriaga 2002; Theuns et al. 2002b). In this paper, we have focused entirely on the thermal state of fluid elements at the mean density. The formalism of Hui & Gnedin (1997) can be used to compute the same for elements at  $\delta\rho/\rho \lesssim 10$ . It is interesting to explore how the variation of temperature with density ( $T \propto \rho^{\gamma-1}$ , an effective equation of state) might place additional constraints on the reionization history. At present, measurements of  $\gamma$  are quite noisy (see, e.g., ZHT01). New approaches to constrain it better will therefore be very useful (M. Dijkstra, A. Lidz, & L. Hui 2003, in preparation). Finally, there is the issue of exotic ionization mechanisms (see, e.g., Berezhiani & Khlopov 1990), which is particularly interesting in the face of early reionization.

We thank Renyue Cen, Andrea Ferrara, Wayne Hu, Avi Loeb, Jerry Ostriker, Joop Schaye, and especially Adam Lidz for useful discussions. We are grateful to the referee for useful comments. L. H. is supported in part by an Outstanding Junior Investigator Award from the DOE, an AST 00-98437 grant from the NSF, the DOE at Fermilab, and NASA grant NAG 5-10842.

## APPENDIX

Here we describe briefly the equations that need to be solved for the thermal and chemical evolution of the IGM. The equations are standard, and much more detail is provided in Hui & Gnedin (1997).

The thermal evolution is dictated by

$$\frac{dT}{dt} = -2HT + \frac{2T}{3(1+\delta)} \frac{d\delta}{dt} - \frac{T}{\sum_i \tilde{X}_i} \frac{d\sum_i \tilde{X}_i}{dt} + \frac{2}{3k_B n_b} \frac{dQ}{dt}, \quad (\text{A1})$$

where  $T$  is the gas temperature of the fluid element of interest,  $H$  is the Hubble parameter,  $d/dt$  is the Lagrangian derivative with respect to proper time, and  $n_b$  is the proper number density of all gas particles (i.e., exclude noninteracting dark matter). The symbol  $\tilde{X}_i$  is defined by  $n_i \equiv (1+\delta)\tilde{X}_i(\bar{\rho}_b/m_p)$ , where  $n_i$  is the proper number density of the species  $i$ ,  $\bar{\rho}_b$  is the mean mass density of baryons at the time of interest,  $m_p$  is the mass of the proton, and  $\delta$  is the mass overdensity. For example, the neutral fraction of hydrogen  $X_{\text{H I}}$  (to be distinguished from  $\tilde{X}_{\text{H I}}$ ) is then  $\tilde{X}_{\text{H I}}/(\tilde{X}_{\text{H I}} + \tilde{X}_{\text{H II}})$ .

The first two terms on the right-hand side take care of adiabatic cooling or heating. The third accounts for the change of internal energy per particle due to the change in the number of particles. The last term  $dQ/dt$  is the heat gain (or negative heat loss) per unit volume by the gas particles from the surrounding radiation field. The heating and cooling rates due to photoionization and recombination (of hydrogen and helium) and Compton scattering are summarized in the appendix of Hui & Gnedin (1997).

The thermal evolution equation has to be supplemented by one that determines the chemical evolution, which takes the form

$$\frac{d\tilde{X}_i}{dt} = -\tilde{X}_i\Gamma_i + \sum_{j,k} \tilde{X}_j\tilde{X}_k R_{jk} \left[ \frac{\bar{\rho}_b(1+\delta)}{m_p} \right], \quad (\text{A2})$$

where  $\Gamma_i$  is the photoionization rate of the species  $i$  and  $R_{jk}$  is the recombination rate (in units of volume per unit time) of the

species  $j$  and  $k$  to give  $i$ . The photoionization rate is given by

$$\Gamma_i = \int_{\nu_i}^{\infty} 4\pi J_\nu \sigma_i \frac{d\nu}{h\nu}, \quad (\text{A3})$$

where  $J_\nu$  is the specific intensity of the ionizing radiation as a function of frequency  $\nu$ ,  $\nu_i$  is the frequency above which a photon can ionize the specie  $i$ , and  $\sigma_i$  is the cross section for this process. The cross sections for different species as well as the recombination rates are given in the appendix of Hui & Gnedin (1997).

What remains to be specified is the time evolution of the specific intensity of the ionizing radiation as a function of frequency, which determines the photoionization ( $\Gamma_i$ ) and photoionization heating ( $dQ/dt$ ) rates. This is of course what determines the reionization history of the universe.

It is perhaps useful to display as an example one term that arises in  $dQ/dt$ , namely, the one due to photoheating of hydrogen:

$$\frac{dQ}{dt} [\text{H I heating}] = n_{\text{H I}} \int_{\nu_{\text{HI}}}^{\infty} 4\pi J_\nu \sigma_{\text{H I}} (h\nu - h\nu_{\text{HI}}) \frac{d\nu}{h\nu}. \quad (\text{A4})$$

Note that, in this paper, we focus exclusively on fluid elements at mean density for simplicity,  $\delta = 0$ , in which case there is no need to have a separate equation that determines the dynamical evolution of  $\delta$ . The thermal and chemical evolution equations are evolved numerically forward from pre-reionization to post-reionization. The results are the various thermal evolution curves shown in our paper.

#### REFERENCES

- Abel, T., & Haehnelt, M. G. 1999, *ApJ*, 520, L13  
 Adelberger, K. L., Steidel, C. C., Shapley, A. E., & Pettini, M. 2003, *ApJ*, 584, 45  
 Anderson, S. F., Hogan, C., Williams, B., & Carswell, R. F. 1999, *AJ*, 117, 56  
 Barkana, R. 2002, *NewA*, 7, 85  
 Becker, R. H., et al. 2001, *AJ*, 122, 2850  
 Berezhiani, Z. G., & Khlopov, M. Y. 1990, *Soviet J. Nucl. Phys.*, 52, 60  
 Bernardi, M., et al. 2003, *AJ*, 125, 32  
 Bromm, V., Kudritzki, R. P., & Loeb, A. 2001, *ApJ*, 552, 464  
 Bryan, G., & Machacek, M. 2000, *ApJ*, 534, 57  
 Burles, S., Nollett, K. M., & Turner, M. S. 2001, *ApJ*, 552, L1  
 Cen, R. 2003, *ApJ*, 591, 12  
 Cen, R., & McDonald, P. 2002, *ApJ*, 570, 457  
 Cowie, L. L., Barger, A. J., Bautz, M. W., Brandt, W. N., & Garmire, G. P. 2003, *ApJ*, 584, L57  
 Croft, R. A. C., Weinberg, D. H., Katz, N., & Hernquist, L. 1997, *ApJ*, 488, 532  
 Dave, R., & Tripp, T. M. 2001, *ApJ*, 553, 528  
 Dijkstra, M., Lidz, A., & Hui, L. 2003, *ApJ*, submitted (astro-ph/0305498)  
 Djorgovski, S. G., Castro, S. M., Stern, D., & Mahabal, A. 2001, *ApJ*, 560, L5  
 Dodelson, S. 2003, *Modern Cosmology* (New York: Academic Press)  
 Fan, X., Narayanan, V. K., Strauss, M. A., White, R. L., Becker, R. H., Pentericci, L., & Rix, H.-W. 2002, *AJ*, 123, 1247  
 ———. 2003, *AJ*, 125, 1649  
 Gnedin, N. Y. 2000, *ApJ*, 535, 530  
 ———. 2001, *MNRAS*, submitted (astro-ph/0110290)  
 Gnedin, N. Y., & Ostriker, J. P. 1997, *ApJ*, 486, 581  
 Gunn, J. E., & Peterson, B. A. 1965, *ApJ*, 142, 1633  
 Haardt, F., & Madau, P. 1996, *ApJ*, 461, 20  
 Haehnelt, M. G., & Steinmetz, M. 1998, *MNRAS*, 298, L21  
 Haiman, Z., & Holder, G. 2003, *ApJ*, 595, 1  
 Haiman, Z., & Loeb, A. 1997, *ApJ*, 483, 21  
 ———. 1998, *ApJ*, 503, 505  
 Heap, S. R., Williger, G. M., Smette, A., Hubeny, I., Sahu, M. S., Jenkins, E. B., Tripp, T. M., & Winkler, J. N. 2000, *ApJ*, 534, 69  
 Hui, L., Burles, S., Seljak, U., Rutledge, R. E., Magnier, E., & Tytler, D. 2001, *ApJ*, 552, 15  
 Hui, L., & Gnedin, N. Y. 1997, *MNRAS*, 292, 27  
 Hui, L., & Rutledge, R. E. 1999, *ApJ*, 517, 541  
 Jakobsen, P., Jansen, R. A., Wagner, S., & Reimers, D. 2003, *A&A*, 397, 891  
 Kogut, A., et al. 2003, *ApJS*, 148, 161  
 Kriss, G. A., et al. 2001, *Science*, 293, 1112  
 Leitherer, C., et al. 1999, *ApJS*, 123, 3  
 Lidz, A., Hui, L., Zaldarriaga, M., & Scoccimarro, R. 2002, *ApJ*, 579, 491  
 Madau, P., & Efstathiou, G. 1999, *ApJ*, 517, L9  
 McDonald, P., Miralda-Escudé, J., Rauch, M., Sargent, W. L. W., Barlow, T. A., Cen, R., & Ostriker, J. P. 2001, *ApJ*, 562, 52 (MM01)  
 Meiksin, A., Bryan, G., & Machacek, M. 2001, *MNRAS*, 327, 296  
 Miralda-Escudé, J., Haehnelt, M., & Rees, M. J. 2000, *ApJ*, 530, 1  
 Miralda-Escudé, J., & Rees, M. J. 1994, *MNRAS*, 266, 343  
 Nakamoto, T., Umemura, M., & Susa, H. 2001, *MNRAS*, 321, 593  
 Oh, S. P. 2001, *ApJ*, 553, 499  
 Rauch, M., Sargent, W. L. W., Barlow, T. A., & Carswell, R. F. 2001, *ApJ*, 562, 76  
 Razoumov, A. O., Norman, M. L., Abel, T., & Scott, D. 2002, *ApJ*, 572, 695  
 Reimers, D., Kohler, S., Wisotski, L., Groote, D., Rodriguez-Pascual, P., & Wamsteker, W. 1997, *A&A*, 327, 890  
 Ricotti, M., Gnedin, N. Y., & Shull, J. M. 2000, *ApJ*, 534, 41  
 Schaerer, D. 2002, *A&A*, 382, 28  
 Schaye, J., Theuns, T., Rauch, M., Efstathiou, G., & Sargent, W. L. W. 2000, *MNRAS*, 318, 817 (ST00)  
 Shapiro, P. R., Giroux, M. L., & Babul, A. 1994, *ApJ*, 427, 25  
 Sokasian, A., Abel, T., & Hernquist, L. 2002, *MNRAS*, 332, 601  
 Songaila, A. 1998, *AJ*, 115, 2184  
 Songaila, A., & Cowie, L. L. 2002, *AJ*, 123, 2183  
 Spergel, D. N., et al. 2003, *ApJS*, 148, 175  
 Tegmark, M., Silk, J., & Blanchard, A. 1994, *ApJ*, 420, 484  
 Theuns, T., Schaye, J., Zaroubi, S., Kim, T. S., Tzanavaris, P., & Carswell, B. 2002a, *ApJ*, 567, L103  
 Theuns, T., Zaroubi, S., Kim, T. S., Tzanavaris, P., & Carswell, B. 2002b, *MNRAS*, 332, 367  
 Tumlinson, J., & Shull, J. M. 2000, *ApJ*, 528, L65  
 Valageas, P., & Silk, J. 1999, *A&A*, 347, 1  
 Venkatesan, A., Giroux, M. L., & Shull, J. M. 2001, *ApJ*, 563, 1  
 Venkatesan, A., Tumlinson, J., & Shull, J. M. 2003, *ApJ*, 584, 621  
 Wyithe, S., & Loeb, A. 2003, *ApJ*, 586, 693  
 Zaldarriaga, M. 2002, *ApJ*, 564, 153  
 Zaldarriaga, M., Hui, L., & Tegmark, M. 2001, *ApJ*, 557, 519 (ZHT01)  
 Zheng, W., Kriss, G., Telfer, R., Grimes, J. P., & Davidsen, A. F. 1998, *ApJ*, 492, 855  
 Zuo, L., & Phinney, E. S. 1993, *ApJ*, 418, 28